

Thermal analysis of induction and synchronous reluctance motors

Original

Thermal analysis of induction and synchronous reluctance motors / Boglietti, Aldo; Cavagnino, Andrea; Pastorelli, MICHELE ANGELO; Vagati, Alfredo; Staton, D.. - In: IEEE TRANSACTIONS ON INDUSTRY APPLICATIONS. - ISSN 0093-9994. - STAMPA. - 42:(2006), pp. 675-680. [10.1109/TIA.2006.873668]

Availability:

This version is available at: 11583/1404626 since:

Publisher:

IEEE

Published

DOI:10.1109/TIA.2006.873668

Terms of use:

This article is made available under terms and conditions as specified in the corresponding bibliographic description in the repository

Publisher copyright

(Article begins on next page)

Thermal Analysis of Induction and Synchronous Reluctance Motors

Aldo Boglietti, *Member, IEEE*, Andrea Cavagnino, *Member, IEEE*, Michele Pastorelli, David Staton, *Member, IEEE*, and Alfredo Vagati, *Fellow, IEEE*

Abstract—In this paper, the thermal behavior of two induction motors (2.2 and 4 kW, four poles) and two synchronous reluctance motors [(SynRMs) transverse-laminated] are investigated and compared. Both motor types use the same stator but have different rotors. Using a lumped-parameter simulation program, a thermal analysis has been also carried out, and the obtained results have been compared with the experimental ones. A direct comparison of the thermal behavior of the two motor types has thus been made for constant load and constant average copper temperature conditions. Inasmuch as the SynRM has negligible rotor losses compared with the induction motor, it is capable of a larger rated torque, from 10% to more than 20%, depending on the relative size of end connections and motor length.

Index Terms—Induction motors, synchronous reluctance motors (SynRMs), thermal model.

I. INTRODUCTION

INDUCTION motors are the worldwide most common drive for industrial and civil applications. This is largely due to their simple construction and robustness and the fact that they can operate directly from the sinusoidal supply without the need of power electronics converter and related control system. Obviously, the last advantage is not valid when the application requires speed regulation. In such a case, there could be many advantages in adopting alternative motor typologies. When choosing a motor type suitable for variable speed drives, characteristics such as high torque/volume ratio, high efficiency, simple controllability, and feasibility of sensorless control are often desired. In the last 10 years, the synchronous reluctance motors (SynRMs) have gained interest [3]–[5] due to several factors:

- reduced cost with respect to permanent-magnet (PM) machines;
- quite simple production and assembly process, even if the rotor lamination geometry shows flux barriers (Fig. 1);
- flux weakening capability for spindle and traction applications.

Paper IPCSD-06-013, presented at the 2005 IEEE International Electric Machines and Drives Conference, San Antonio, TX, May 15–18, and approved for publication in the IEEE TRANSACTIONS ON INDUSTRY APPLICATIONS by the Electric Machines Committee of the IEEE Industry Applications Society. Manuscript submitted for review May 23, 2005 and released for publication February 23, 2006.

A. Boglietti, A. Cavagnino, M. Pastorelli, and A. Vagati are with the Dipartimento di Ingegneria Elettrica Industriale, Politecnico di Torino, 10129 Turin, Italy (e-mail: aldo.boglietti@polito.it; andrea.cavagnino@polito.it; michele.pastorelli@polito.it; alfredo.vagati@polito.it).

D. Staton is with Motor Design Ltd., Ellesmere, SY12 9DA, U.K. (e-mail: dave.staton@motor-design.com).

Digital Object Identifier 10.1109/TIA.2006.873668

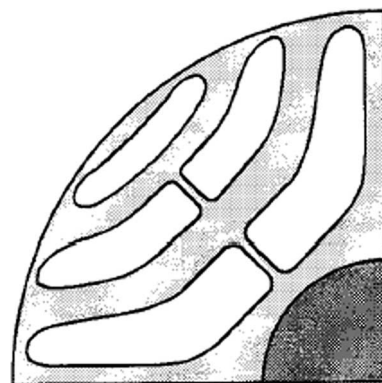


Fig. 1. Schematic of rotor lamination of a transverse-laminated SynRM.

Inasmuch as there are no rotor losses in the SynRM, this motor has a cooler rotor compared with that of the induction motor. This allows higher efficiency and reduced problems related to bearing temperature.

The SynRM suited for mass production is the transverse-laminated one. It is composed of a three-phase stator (a common induction motor stator can be employed), whereas the rotor is realized by a multiple-barrier structure, traditionally laminated.

As a schematic example, Fig. 1 shows a SynRM rotor lamination of a four-pole motor. The thin ribs connecting the flux guides are designed to withstand the centrifugal forces produced at high speed.

Due to the different rotor laminations and the absence of rotor currents, the thermal behavior of the SynRM differs from the behavior of the induction motor. The analysis of the thermal behaviors is carried out both by simulation models and experimental validation.

II. THERMAL ANALYSIS AND COMPARISON

To compare the thermal behavior of a SynRM to that of an induction motor, both thermal analysis by a simulation package and experimental tests have been carried out. The comparison has been performed using induction and SynRM motors produced by the same company, having the same stators. Thus, the difference in the motor performance is due only to the rotor lamination. The motors adopted in the analysis are totally enclosed fan-cooled (TEFC) induction motors, with 2.2- and 4-kW rated power (380 V, 50 Hz, four poles, F insulation class). The SynRMs have been equipped with encoders for the closed-loop control. As an example, Fig. 2 is a photograph of the 4-kW motor.

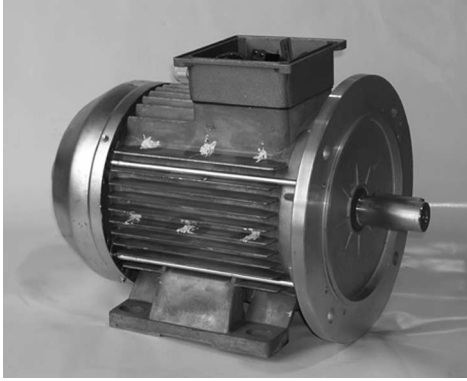


Fig. 2. TEFC 4-kW (380 V, 50 Hz, four poles) induction motor.

The step-by-step analysis has been developed in the following way:

- induction motor tests;
- induction motor thermal simulation and thermal model setup;
- SynRM motor thermal simulation;
- thermal comparison between SynRM simulation and experimental results;
- comparison between SynRM and induction motor performance.

III. INDUCTION MOTOR TEST

Several tests have been performed on the two induction motors. In particular, the following tests have been chosen for the thermal characterization.

A. Load Test With AC Inverter Supply

This test, performed at rated load, allows to define the steady-state thermal conditions. The temperatures of the frame and stator iron have been measured by thermal probes.

The winding average temperature has been measured through dc supply. It is important to underline that all the motors have been monitored with thermocouples on the end windings, whereas the iron temperatures have been measured through a hole drilled on the motor frame. The frame temperatures have been measured, at several points, on the motor frame surface, and an average temperature value has been used for the subsequent analysis. During the load test, all the measurable electrical and mechanical quantities have been monitored. The measured values have been used for the loss segregation using the procedure proposed by the IEEE 112 method B. Although this method is a standard procedure for sinusoidal supply, it is possible to apply it to an inverter supply if some simplified hypotheses are introduced. Inasmuch as the quantities are related to inverter supply, all the measured and computed powers have to be total active powers, whereas the related voltages have to be the first harmonic of the applied inverter voltages. The additional losses have been neglected for two reasons.

- 1) The additional losses are small with respect to the other contributions, and their effect on the thermal behavior can be neglected, for simplicity.

- 2) The IEEE procedure is for sinusoidal supply. As well known, the additional losses are related to the effects of the space harmonics content on the rotor cage. With inverter supply, new additional losses due to supply are involved (in particular, voltage and current time harmonics components). Anyway, these losses are automatically included in the loss balance using the measured root-mean-square (rms) current values. Consequently, there is not a simple and reliable procedure to separate these two contributions.

During the load test, a map of the cooling airspeed on the motor frame surface has been determined by means of an anemometer probe. These data have been used to calibrate the thermal simulation. A complete discussion on the problems linked to the airspeed measurements in TEFC motors can be found in [2] and [6].

B. No-Load Test With AC Inverter Supply

This test allows evaluation of core loss and mechanical loss. Both losses are requested in the IEEE 112 Method B loss separation, and they have to be known in the thermal model setup.

C. Thermal Test With DC Supply

This test is performed with the motor supplied by a dc voltage and is the base for the thermal model setup. The data collected by this test are used to determine the following:

- equivalent thermal conductivity of the impregnation varnish (considering an impregnation goodness equal to 1);
- interface gap between stator core and motor frame;
- natural convection heat-transfer coefficient.

These three quantities are of fundamental relevance for a correct setup of the thermal model. The thermal set procedure is described in [2] and [6]. Anyway, a short summary is hereafter reported.

During the dc test, the shaft is still, and the fan cooling is not active. Therefore, to avoid a motor damage, the current has to be regulated between 40%–60% of the rated one.

The test starts by measuring the motor resistance at the ambient temperature, thus constituting the reference value. When the motor reaches the steady-state temperature, the external housing temperatures are measured in different points (Fig. 3) to get the average housing temperature. In addition, an internal temperature is also measured up to the stator iron. Lastly, the new value of the stator resistance is measured, and the motor winding temperature is computed by the trivial relationship (1)

$$T_2 = (235 + T_1) \frac{R_2}{R_1} - 235 \quad (1)$$

where

- T_1 ambient temperature;
- R_1 stator resistance at ambient temperature;
- R_2 stator resistance at temperature T_2 .

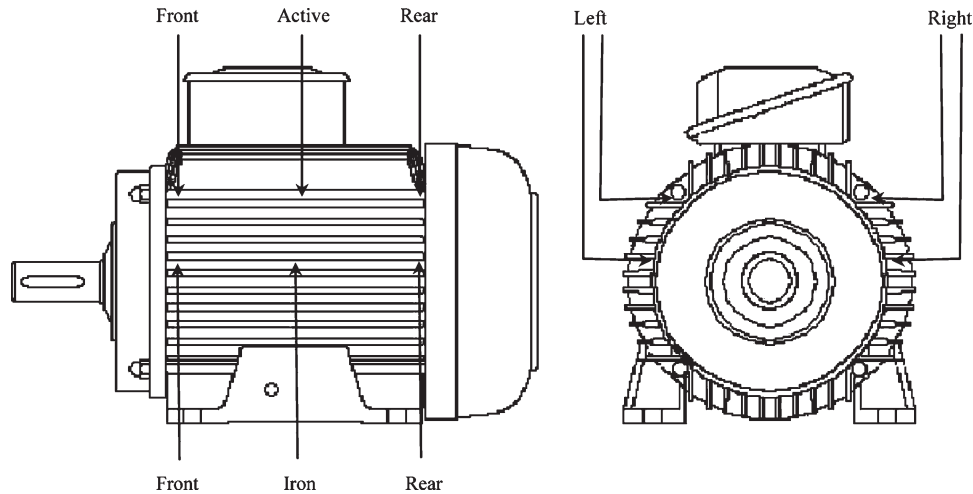


Fig. 3. Temperature measurement points.

TABLE I
INDUCTION MOTOR 2.2 kW

	Overtemperatures [°C]			
	DC Test		AC Test	
	Exper.	Simul.	Exper.	Simul.
Housing	35.5	37.0	38.8	47.0
Stator iron	37.6	40.4	49.0	74.9
Winding average	46.1	46.2	102.8	102.1

TABLE II
INDUCTION MOTOR 4 kW

	Overtemperatures [°C]			
	DC Test		AC Test	
	Exper.	Simul.	Exper.	Simul.
Housing	48.3	52.9	61.5	60.9
Stator iron	53.2	57.5	72.6	92.9
Winding average	61.6	61.3	106.8	107.0

IV. SETUP OF THE INDUCTION MOTOR THERMAL MODEL AND SIMULATIONS

The induction motor model setup and the thermal simulations have been performed using the commercial software package Motor-CAD¹ that is a code devoted to electrical motor thermal analysis [1]. The implemented model is based on an analytical lumped circuit. The comparison between the simulated and the measured overtemperatures are reported in Tables I and II, for both the dc test and the ac load test, respectively. Fig. 4 shows the test bench for the ac tests.

With reference to Tables I and II, the dc tests have been performed with a current of 40%–50% lower than the rated one to keep the overtemperature less than the maximum because the motor is not running and the fan cooling effect is absent. The ac tests have been performed at rated torque (2.2 kW, $T = 15.1 \text{ N} \cdot \text{m}$, $n = 1200 \text{ r/min}$; 4 kW, $T = 27.4 \text{ N} \cdot \text{m}$, $n = 1100 \text{ r/min}$).

The dc tests are matched, of course, because they have been used to set up the model. Regarding the ac tests, a fairly good matching is shown for winding and housing temperatures. On

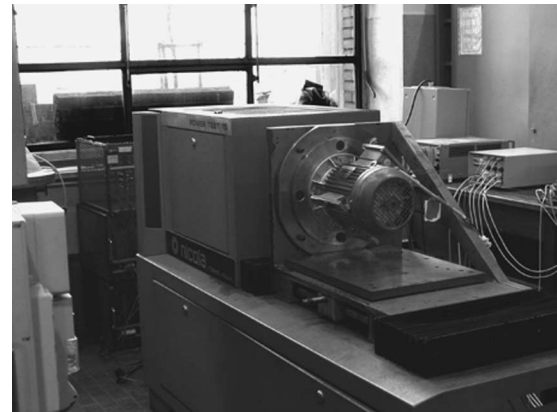


Fig. 4. Test bench for the ac load test.

the contrary, a discrepancy is pointed out regarding the iron temperature.

In order not to damage the stator lamination, as previously reported, the drilled hole has been limited to the motor frame. Therefore, the measured temperature would be intermediate between iron and stator frame because a thermocouple probe with silicon grease was used. Of course, other concurrent explanations can be found. Anyway, the impact of this discrepancy on the following comparison is limited because it is mainly based on the copper temperature.

During the ac load test, the dissipative effect of the test bench has to be taken into account. In fact, the metal structure of this bench (Fig. 3) cannot be neglected. As discussed in Section III, the dc test was performed on the motor alone, to get the thermal characteristic of the motor only. To take into account the presence of the test bench in the thermal model because the software code allows the inclusion of a rectangular flange with dimensions imposed by the user, a flange equivalent to the test bench was introduced.

An additional dc test with the motor mounted on the bench has been performed, similarly to the dc test without bench (Section III). Thus, using the thermal model previously set up, the flange dimension is modified until the predicted temperatures cope the measured ones. The use of a thermal equivalent

¹Motor-CAD. [Online]. Available: www.motor-design.com

TABLE III
SYNRM 2.2 kW ($T = 15.1 \text{ N} \cdot \text{m}$, $n = 1200 \text{ r/min}$)

Overtemperatures [°C]		
	AC Test	
	Exper.	Simul.
Housing	39.8	37.4
Stator iron	44.1	60.0
Winding average	85.0	85.0

TABLE IV
SYNRM 4 kW ($T = 27.4 \text{ N} \cdot \text{m}$, $n = 1100 \text{ r/min}$)

Overtemperatures [°C]		
	AC Test	
	Exper.	Simul.
Housing	42.9	47.8
Stator iron	47.6	64.4
Winding average	79.0	80.9

flange in the model leads to an excellent agreement between the measured and predicted motor temperatures, as shown in Tables I and II. It can be pointed out that the described procedure (two dc tests with and without bench) has the advantage of overcoming the difficult evaluation of the thermal characteristics of the real flange.

V. SYNRM MOTOR THERMAL MODEL

The thermal behavior of the SynRM has been carried out using the software code adopted for the induction motor analysis. However, this software does not provide an *ad hoc* thermal model for SynRMs. Therefore, the thermal model used for the induction motor has been adapted to the SynRM. Taking into account that the main difference between the two motors is the rotor structure, four approximations were adopted.

- 1) Rotor losses were set to zero.
- 2) Thermal conductivity of the rotor cage was set equal to the thermal conductivity of the air.
- 3) Difference between the thermal resistances of the two rotors was neglected.
- 4) Inasmuch as bearings and fans are equal and the two motors are supplied by the same inverter, mechanical and iron losses have been assumed equal for the two motors.

The obtained SynRM thermal model has been used to analyze the two SynRMs under test, as described in the following.

VI. THERMAL COMPARISON BETWEEN SIMULATION AND EXPERIMENTAL RESULTS ON SYNRM

As a first step, the two SynRMs have been tested at load and at the same torque and shaft speed of the two the induction motors.

At steady state, the SynRM temperatures have been measured and compared with the temperatures obtained from the SynRM thermal model previously discussed.

The comparison is reported in Tables III and IV. The two tables show a fairly good agreement between the measured and the predicted values, with reference to winding and housing temperatures. As usual, a discrepancy is found for the stator iron temperature, but the considerations concerning the hole drilled in the stator frame and the temperature probe insertion are still valid.

TABLE V
SYNRM 2.2 kW—OVERLOAD ($16.4 \text{ N} \cdot \text{m}$, 1200 r/min)

Overtemperatures [°C]		
	Exper.	Simul.
Winding average	103.4	103

TABLE VI
SYNRM 4 kW—OVERLOAD ($32.9 \text{ N} \cdot \text{m}$, 1100 r/min)

Overtemperatures [°C]		
	Exper.	Simul.
Winding average	108.6	107.6

TABLE VII
CONSTANT TORQUE AND SHAFT SPEED:
RATIO OF DISSIPATED POWERS

	2.2 kW	4 kW
Pdr/Pdi	.83	0.73

VII. INDUCTION VERSUS SYNRM

On the basis of the previous results, it is possible to compare induction and SynRMs from the thermal point of view by using the winding average temperatures shown in Tables I–IV. As expected, it is well evident that the SynRMs are cooler than induction motors, at the same load conditions. In particular, a reduction of about 14°C has been found for the 2.2-kW motors and of 28°C for the 4-kW motors. A rotor without joule losses is a considerable advantage for the SynRM, which leads to a consistent reduction of the winding temperature at the same load torque and speed. Therefore, rather than using the SynRMs at a lower temperature, an increase of the rated torque to get the same temperature of the induction motor is a viable and profitable approach. This can be obtained by increasing the torque current component. In other words, at constant stator winding temperature, the SynRMs show higher rated torque; this load condition can be briefly pointed as “overload.” As far as mechanical and stator iron losses can be considered independent with respect to the motor torque, the stator copper losses (i.e., the stator current) can be increased until the winding temperatures of the SynRMs match the temperature of the induction motors. This procedure has been applied both by simulation using the thermal model and by direct load tests. With reference to the winding temperature, Tables V and VI show the comparison between simulated and measured results.

Both tables show a good agreement between predicted and simulated results, confirming the reliability of the proposed SynRM thermal model. The temperatures of Tables V and VI have to be compared with the ones reported in Tables I and II.

The ratio between the power dissipations of the two motors (Pdi for the induction motors and Pdr for the SynRMs) at constant torque and shaft speed Pdi/Pdr and the ratio between the two torques (Ti for the induction motors and Tr for the SynRMs) at constant average winding temperature Tr/Ti can be evaluated. These ratios are reported in Tables VII and VIII.

At constant load, the power dissipation of the induction motors is 20%–37% higher than that of the SynRMs. On the other hand, when the same power dissipation is imposed, the torque of the SynRM is 10%–20% larger than that of the induction motor.

TABLE VIII
CONSTANT AVERAGE WINDING OVERTEMPERATURE:
RATIO OF OUTPUT TORQUES

	2.2 kW	4 kW
Tr/Ti	1.09	1.20
Ir/Ii	1.11	1.24

TABLE IX
MAIN DIMENSIONS OF THE MOTOR FRAMES (IN MILLIMETERS)

	D.ext	D.int	l
2.2 kW	165	98	70
4 kW	165	98	120

The quite different amount of torque increasing, between 2.2- and 4-kW motors, can be surprising. It is explained by the quite different impact of end connections. The main motor dimensions are reported in Table IX, where D.ext is the stator lamination outer diameter, D.int is the stator lamination bore diameter, and l is the stack length.

It is important to highlight that the 2.2-kW motor has a low value of the ratio of stack length over external diameter ($l/D.ext$). Inasmuch as the extra torque of the SynRM is due to a transfer of the induction motor rotor losses, the shorter the motor is, the lower this transfer is, because the large loss amount due to end connections does not contribute to torque production.

Moreover, consider that even the 4-kW motors can still be considered “short” motors. Therefore, a larger torque increase could be expected for a longer motor.

In principle, for a motor of infinite length, all the induction motor rotor losses could be transferred to the stator, and a maximum torque increase would be reached. In practice, however, only a portion of these losses is useful to increase the torque capability.

This point has been analyzed in detail using the simulation program. The obtained results have shown the peculiarities of the thermal dissipation of the stator end windings, in comparison to the active section of the windings inside the stator slots. In particular, the end windings have a high thermal resistance between the two end bells and the external frame. By the simulation program, the maximum temperature values of end connections have been calculated for both the considered motor frames and for both motor types. In the worst case, the maximum temperature is higher than the average one by 12 °C, which looks reasonable. On the other hand, by comparing the highest temperatures of synchronous reluctance and induction motors, the former was typically showing 3 °C more than the latter. This confirms the validity of the previous comparison based on the average temperature values.

A way to reduce the impact of end connections should be the adoption of potted end windings [7], as shown in Fig. 5. The thermal simulation code previously used has been also applied to this case, and the obtained results are shown in Table X.

A material with a thermal conductivity of about 1 W/°C/m has been supposed. Both the induction motor and the SynRM have been simulated because the potted ends are profitable in both cases.

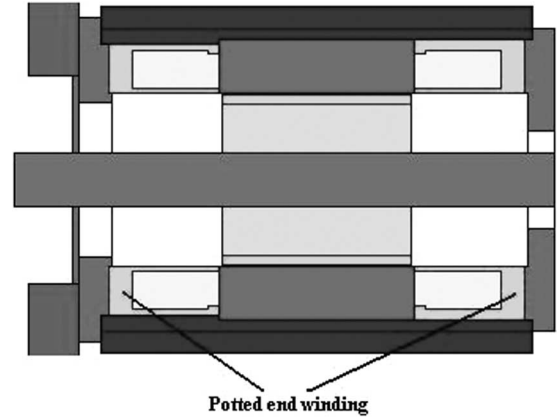


Fig. 5. Example of potted end windings.

TABLE X
RATED CURRENT RATIO (SYNRM CURRENT OVER
INDUCTION MOTOR CURRENT)

Constant average winding temperature		
	2.2 kW	4 kW
non potted end windings	1.10	1.22
potted end windings	1.13	1.23

As a result, the ratios given by Table X were found. They represent the rated current of the SynRM referred to the induction motor one, at the same average winding temperature. As expected, the shorter motor improves its performance more than the other one. Anyway, the impact of potted ends looks quite limited, with reference to our comparison. On the other hand, the difference between maximum and average temperatures is limited, in this case, to few degrees; this constitutes an advantage, in general.

VIII. CONCLUSION

In this paper, a direct comparison between induction motors and SynRMs has been presented. A simplified thermal model of the SynRM has been proposed. The comparison between the predicted and the measured results has shown a good agreement, with main reference to the stator winding temperature.

The obtained results have highlighted the quite higher torque density of the modern SynRM with respect to the standard induction motor. Due to its negligible rotor losses, the SynRM shows a rated torque, which is from 10% to 20% larger, depending on the ratio between stack length and stator diameter. Lastly, the impact of potted windings on this comparison has been quantified.

REFERENCES

- [1] D. Staton, A. Boglietti, and A. Cavagnino, “Solving the more difficult aspects of electric motor thermal analysis in small and medium size industrial induction motors,” *IEEE Trans. Energy Convers.*, vol. 20, no. 3, pp. 620–628, Sep. 2005.
- [2] A. Boglietti, A. Cavagnino, and D. Staton, “Thermal analysis of TEFC induction motors,” in *Conf. Rec. IEEE-IAS Annu. Meeting*, Salt Lake City, UT, Oct. 12–16, 2003, pp. 849–856.
- [3] A. Vagati, A. Fratta, G. Franceschini, and P. M. Rosso, “A.C. motor for high-performance drives: A design-based comparison,” *IEEE Trans. Ind. Appl.*, vol. 32, no. 4, pp. 1211–1219, Sep./Oct. 1996.

- [4] G. Franceschini, A. Fratta, C. Petrache, A. Vagati, and F. Villata, "Design comparison between induction and synchronous reluctance motors," in *Proc. ICEM*, Paris, France, Sep. 6–8, 1994, pp. 329–334.
- [5] A. Vagati, A. Canova, P. Guglielmi, and M. Pastorelli, "Design and control of high performance synchronous reluctance motor with multiple-flux-barrier rotor," in *Proc. IPEC*, Tokyo, Japan, Apr. 3–7, 2000, vol. 1, pp. 627–636.
- [6] A. Boglietti, A. Cavagnino, and D. Staton, "TEFC induction thermal models: A parameters sensitivity analysis," *IEEE Trans. Ind. Appl.*, vol. 41, no. 3, pp. 756–763, May/Jun. 2005.
- [7] D. A. Staton and E. So, "Determination of the optimal thermal parameters for brushless permanent magnet motor design," in *Conf. Rec. IEEE-IAS Annu. Meeting*, St. Louis, MO, Oct. 1998, vol. 1, pp. 41–49.



Aldo Boglietti (M'04) was born in Rome, Italy, in 1957. He received the Laurea degree in electrical engineering from the Politecnico di Torino, Turin, Italy, in 1981.

He started his research work with the Department of Electrical Engineering, Politecnico di Torino, as a Researcher of electrical machines in 1984. He was an Associate Professor of electrical machines in 1992 and has been a Full Professor since November 2000. He is the Head of the Department of Electrical Engineering and will be holding the position until 2007.

He is the author of about 100 papers. His research interests include energetic problems in electrical machines and drives, high-efficiency industrial motors, magnetic materials and their applications in electrical machines, electrical machine and drive models, and thermal problems in electrical machines.



Andrea Cavagnino (M'04) was born in Asti, Italy, in 1970. He received the M.Sc. and Ph.D. degrees in electrical engineering from the Politecnico di Torino, Turin, Italy, in 1995 and 1999, respectively.

Since 1997, he has been with the Electrical Machines Laboratory, Department of Electrical Engineering, Politecnico di Torino, where he is currently an Assistant Professor. He has authored several papers published in technical journals and conference proceedings. His fields of interest include electromagnetic design, thermal design, and energetic behaviors of electric machines.

Dr. Cavagnino is a Registered Professional Engineer in Italy.



Michele Pastorelli was born in Novara, Italy, in 1962. He received the Laurea and Ph.D. degrees in electrical engineering from the Politecnico di Torino, Turin, Italy, in 1987 and 1992, respectively.

In 1988, he joined the Department of Electrical Engineering, Politecnico di Torino, where he is currently an Associate Professor. He has authored about 70 papers published in technical journals and conference proceedings. His fields of interest include power electronics, high-performance servo drives, and energetic behaviors of electrical machines.

Dr. Pastorelli is a Registered Professional Engineer in Italy.



David Staton (M'97) received the Ph.D. degree in computer-aided design of electrical machines from Sheffield University, Sheffield, U.K., in the mid-1980s.

Since then, he has worked on motor design and, in particular, development of motor design software at Thorn EMI, the SPEED Laboratory at Glasgow University, and Control Techniques. In 1999, he set up a new company, Motor Design Ltd., Ellesmere, U.K., to develop thermal analysis software for electrical machines.



Alfredo Vagati (M'88–SM'92–F'98) received the Laurea degree in electrical engineering from the Politecnico di Torino, Turin, Italy, in 1970.

After a few years working in industry with Olivetti, he joined the Politecnico di Torino in 1975 as an Assistant Professor. From 1982 to 1990, he was an Associate Professor of electrical drives. In 1990, he became a Professor of electrical machines and drives at the University of Cagliari, Cagliari, Italy. In 1991, he rejoined the Politecnico di Torino in the same capacity. He was the Chair of the Electrical

Engineering Department of the Politecnico di Torino from 1995 to 2003. His scientific activity, in the field of electrical machines and drives, has particularly concerned high-performance ac drives. He has been involved in several industrial projects, in the field of ac drives, as both a designer and a scientific reference. The most important activity of this kind has concerned design and control of newly developed high-performance synchronous reluctance motors. He has led several countrywide and European research projects, in the field of design and control of synchronous machine-based drives, for different applications, including home appliances and the automotive world. He has authored or coauthored more than 80 technical papers.

Prof. Vagati is a Permanent Member of the Technical Program Committee of the PCIM International Conference and Exhibition. He is also a member of the Industrial Drives and Electric Machines Committees of the IEEE Industry Applications Society.